Chemical Engineering Science 297 (2024) 120292

Contents lists available at ScienceDirect

Chemical Engineering Science

journal homepage: www.elsevier.com/locate/ces

Precision calculation of the entrance length for laminar flow of Bingham fluid between parallel plates with yield number from 0 to 1000

Alexandre Lavrov

Norwegian University of Science and Technology (NTNU), Department of Geoscience and Petroleum, Trondheim, Norway

ARTICLE INFO

Keywords:
Bingham fluid
Flow between parallel plates
Entrance region
Entrance length
Development length
Developed flow

ABSTRACT

An estimate of the entrance length for a Bingham fluid flowing between parallel plates is needed in engineering applications. The dimensionless entrance length is a function of yield number. The primary objective of this study was to construct plots of dimensionless entrance length *vs.* yield number that could be used by practitioners for a quick estimation of the entrance length in a Bingham fluid entering between parallel plates, in a range of yield numbers from 0 to 1000. Three well-known calculation methods were used. The methods were found to yield mutually consistent results. A secondary objective of this study was to examine the sensitivity of the calculated entrance length to the value of a dimensionless parameter somewhat arbitrary chosen during the calculations. This parameter specifies the dimensionless value of the unyielded core velocity that is accepted as the core velocity at the end of the entrance region. In all three calculation methods, the entrance length was found to have a noticeable sensitivity to the variation of this parameter. The least sensitive method was the one based on the momentum integral solution. The findings necessitate further, more fundamental research on the entrance length in non-Newtonian fluids.

1. Introduction

Flow of non-Newtonian yield-stress fluids between parallel plates is encountered in various engineering applications. The Bingham model is commonly used in engineering practice as it is the simplest rheological model that incorporates an essential feature of real yield-stress fluids, *viz.* the existence of a nonzero yield stress (Rodríguez de Castro et al., 2020). Yield stress is the shear stress below which the fluid does not flow.

Fully developed, linear Stokes flow (Re < 1) of a Bingham fluid in the *x*-direction between parallel plates is described by the following solution to the momentum conservation equation (Lipscomb and Denn, 1984):

$$v = \begin{cases} 0 \text{ if } \left|\dfrac{dP}{dx}\right| < \dfrac{\tau_Y}{h} \\ \left(-\dfrac{h^2}{3\mu_{\text{pl}}} + \dfrac{1}{2}\dfrac{h\tau_Y}{\mu_{\text{pl}}\left|dP/dx\right|} - \dfrac{1}{6}\dfrac{\tau_Y^3}{\mu_{\text{pl}}h\left|dP/dx\right|^3} \right)\dfrac{dP}{dx} \text{ if } \left|\dfrac{dP}{dx}\right| > \dfrac{\tau_Y}{h} \end{cases} \quad (1)$$

where h is half the distance between the parallel plates (half the aperture of the channel); dP/dx is the pressure gradient; τ_Y is the yield stress; μ_{pl} is the plastic viscosity. In a fully developed flow, the velocity profile across the aperture consists of three regions: the unyielded core in the middle and the viscous flow regions near the walls (Fig. 1). If the pressure gradient is below τ_Y/h, the entire aperture is occupied by the unyielded core, and there is no flow, cf. Eq. (1_1).

When a Bingham fluid enters a channel, it is commonly assumed to have a uniform velocity profile, and thus all fluid is moving as an unyielded core (Fig. 1). Downstream, the viscous flow region near the walls continually develops until the velocity distribution approaches the theoretical profile that includes an unyielded core and two viscous flow regions. The region from the inlet to where the fully developed velocity distribution is established is called the entrance region. The length of the entrance region is called the entrance length or development length. In practical applications within different branches of engineering, it is important to find an estimate of the entrance length, in order to improve design of laboratory or industrial equipment as well as to ensure realism in numerical simulations. The importance of this issue for non-Newtonian fluids has been recognized for at least five decades, with the earliest attempts back in the 1970s (Batra and Kandasamy, 1990; Das, 1992; Gupta, 1987, 1995b; Nowak and Gajdeczko, 1983; Soto and Shah, 1976; Wilson and Taylor, 1996), which also includes flow in different geometries (Mitsoulis and Huilgol, 2004).

In the previous studies (Batra and Kandasamy, 1990; Gupta, 1995a, b), entrance lengths were evaluated only at few selected values of the

E-mail address: Alexandre.Lavrov@ntnu.no.

https://doi.org/10.1016/j.ces.2024.120292
Received 30 December 2023; Received in revised form 22 April 2024; Accepted 23 May 2024
Available online 25 May 2024

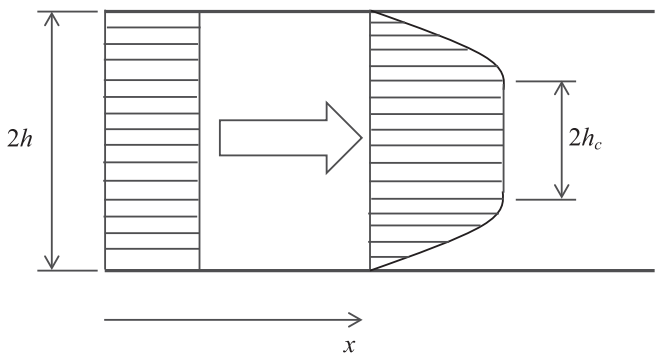

Fig. 1. Schematic illustration of entrance region in a channel. Inlet on the left. Velocity profile at the inlet is uniform. Velocity profile further downstream includes unyielded core moving with constant velocity, and two viscous flow regions. Flow direction is indicated with an arrow. $2h_c$ is the thickness of the unyielded core.

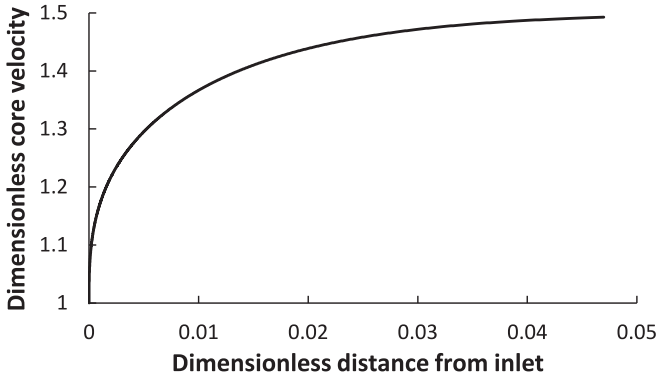

Fig. 2. Example of dimensionless core velocity *vs.* dimensionless distance from the inlet obtained with yield number Bi = 10^{-5}.

yield number, ranging from 0 (Newtonian fluid) to 10. In practice, it is useful to be able to make a quick estimate of the entrance length at any yield number in a wider range. However, as we shall see in Section 2, in order to achieve this, a numerical procedure should be used every time we need to calculate the entrance length. The first objective of this study was therefore to construct graphs that could be used by practitioners for a quick estimation of the entrance length in a channel flow of a Bingham fluid, at a given yield number.

It should be noted that in the entrance region the velocity profile approaches the fully developed profile *asymptotically*. Hence, in theory, the fully developed profile is never reached. Similarly, the core velocity is asymptotically approaching its fully developed value, as shown in Fig. 2 (definitions of dimensionless velocity and dimensionless distance are given in Section 2). It is customary to define the entrance length as the length between the inlet and the location where the velocity of the unyielded core has reached a factor of $\kappa = 0.99$ of its theoretical value it would assume in a fully developed flow (Gupta, 1995b). As part of the present study, the effect of different choices of κ on the predicted entrance length was investigated. The second objective of this study was thus to examine how sensitive the estimated entrance length is to the chosen value of κ, a parameter that is usually set equal to 0.99 for Newtonian and non-Newtonian fluids but whose possible effect on the predicted entrance length is seldom discussed.

2. Methodology

The fluid is assumed to be incompressible. Four dimensionless variables are used when calculating the entrance length: dimensionless distance from the inlet in the direction of flow, dimensionless yield number (Bingham number), dimensionless velocity of the unyielded core, and dimensionless thickness of the unyielded core.

The dimensionless distance from the inlet is defined as

$$\widehat{x} = \frac{x\mu_{\mathrm{pl}}}{4h^2\rho u_0} \tag{2}$$

where x is the distance from the inlet (Fig. 1); ρ is the fluid density; u_0 is the fluid velocity at the inlet. The latter is equal to the average fluid velocity anywhere else in the channel, due to the assumed incompressibility. Defining the Reynolds number for Bingham fluid as $\mathrm{Re} = 2h\rho u_0/\mu_{\mathrm{pl}}$ [this is, up to a constant factor, the same definition of Re as the one used for Bingham fluids e.g. in (Hanks, 1963)], the above definition of dimensionless distance becomes: $\widehat{x} = x/2h\mathrm{Re}$.

Accordingly, the value of $\widehat{x}$ at the downstream end of the entrance region will be called 'the dimensionless entrance length' and denoted by $\widehat{x}_{fd}$ (subscript '*fd*' for 'fully developed').

The yield number is defined as

$$Bi = \frac{\tau_{\mathrm{Y}} w}{2\mu_{\mathrm{pl}} u_0} \tag{3}$$

The dimensionless velocity of the unyielded core is defined as

$$\widehat{u}_c = \frac{u_c}{u_0} \tag{4}$$

where u_c is the velocity of the unyielded core.

The dimensionless half-thickness of the unyielded core is defined as

$$\widehat{h}_c = \frac{h_c}{h} \tag{5}$$

where h_c is half-thickness of the unyielded core (Fig. 1). The dimensionless half-thickness of the unyielded core decreases from 1 at the inlet (where the velocity is uniform) to its value, $h_{c,fd}$, in the fully developed flow. From Eq. (1), the relationship between the yield number and the dimensionless half-thickness of the unyielded core in the fully developed flow is given by:

$$Bi = \frac{6\widehat{h}_{c,fd}}{\left(2+\widehat{h}_{c,fd}\right)\left(1-\widehat{h}_{c,fd}\right)^2} \tag{6}$$

As $\widehat{h}_{c,fd}\to 0$, Bi → 0, and as $\widehat{h}_{c,fd}\to 1$, Bi → ∞, as expected. The core velocity is related to the core thickness as follows (Batra and Kandasamy, 1990):

$$\widehat{u}_c = \frac{3}{2+\widehat{h}_c} \tag{7}$$

From Eqs. (1) and (7), the core thickness at the location where the core velocity is equal to κ times the fully developed core velocity is given by

$$\widehat{h}_{c,\kappa} = \frac{3\left(2-3\widehat{h}_{c,fd}+\widehat{h}_{c,fd}^3\right)}{\kappa\left(3-6\widehat{h}_{c,fd}+3\widehat{h}_{c,fd}^2\right)} - 2 \tag{8}$$

Three methods of calculating the entrance length were described in (Gupta, 1995b): the method based on the momentum integral solution, the method proposed by Batra and Kandasamy in (Batra and Kandasamy, 1990), and the method proposed by Gupta in (Gupta, 1995a). The overall strategy in all three methods is similar: First, given the yield number, the dimensionless half-thickness of the unyielded core in the fully developed flow is found by solving Eq. (6) using Newton's method (exit tolerance in the present study: 10^{-5}). Second, the dimensionless core thickness is evaluated at the location where the core velocity is equal to κ times the fully developed core velocity, using Eq. (8). Finally, the entrance length is evaluated through numerical evaluation of the following integral:

$$\widehat{x}_{\kappa}(\widehat{h}_c) = \int_1^{\widehat{h}_{c,\kappa}} \widehat{x}'(\widehat{h}_c) d\widehat{h}_c \tag{9}$$

where $\widehat{x}'(\widehat{h}_c)$ is derived from the conservation laws. $\widehat{x}'(\widehat{h}_c)$ is always negative because the thickness of the unyielded core decreases from 1 (at the inlet) to the theoretical value found in the fully developed flow (never reaching the latter).

Functions $\widehat{x}'(\widehat{h}_c)$ are specific for each of the three methods mentioned above and are given below. The integral was calculated using Simpson's method with 1000 discretization intervals.

In the method proposed by Batra and Kandasamy, the problem was solved without a pre-assumed velocity profile in the boundary layer resulting in the following $\widehat{x}'vs.\widehat{h}_c$:

$$\widehat{x}'(\widehat{h}_c) = -\frac{-3(2+7\widehat{h}_c)(1-\widehat{h}_c)^2}{5(2+\widehat{h}_c)^2\left[24\widehat{h}_c - 4Bi(2+\widehat{h}_c)(1-\widehat{h}_c)^2\right]} \tag{11}$$

In the method proposed by Gupta, an improved momentum integral equation was obtained by expressing the shear stress using the velocity distribution, resulting in the following $\widehat{x}'vs.\widehat{h}_c$:

$$\widehat{x}'(\widehat{h}_c) = -\frac{3(1-\widehat{h}_c)\left[792 - 648(1-\widehat{h}_c) - 280(1-\widehat{h}_c)^2 + 224(1-\widehat{h}_c)^3\right]}{1120(2+\widehat{h}_c)^2\left\{6\left[2 - 3(1-\widehat{h}_c) + (1-\widehat{h}_c)^2\right] + Bi(2+\widehat{h}_c)(1-\widehat{h}_c)\left[3 - 6(1-\widehat{h}_c) + 2(1-\widehat{h}_c)^2\right]\right\}} \tag{12}$$

The method-specific functions $\widehat{x}'(\widehat{h}_c)$ are as follows (Batra and Kandasamy, 1990; Gupta, 1995a, b). In the method based on the momentum integral solution:

$$\widehat{x}'(\widehat{h}_c) = -\frac{3(13-7\widehat{h}_c)(1-\widehat{h}_c)}{20(2+\widehat{h}_c)^2[6+Bi(2+\widehat{h}_c)(1-\widehat{h}_c)]} \tag{10}$$

Calculations of the entrance length were performed in the 1990s for a few selected values of Bi, e.g. for five Bi values in (Batra and Kandasamy, 1990), including Bi = 0 (Newtonian case), and for two values of Bi in (Gupta, 1995b). In practical applications, the yield number may vary in a wide range. Performing calculations according to the recipe outlined above every time one needs an estimate of the entrance length is somewhat tedious. It would be more convenient to have at hand a plot of

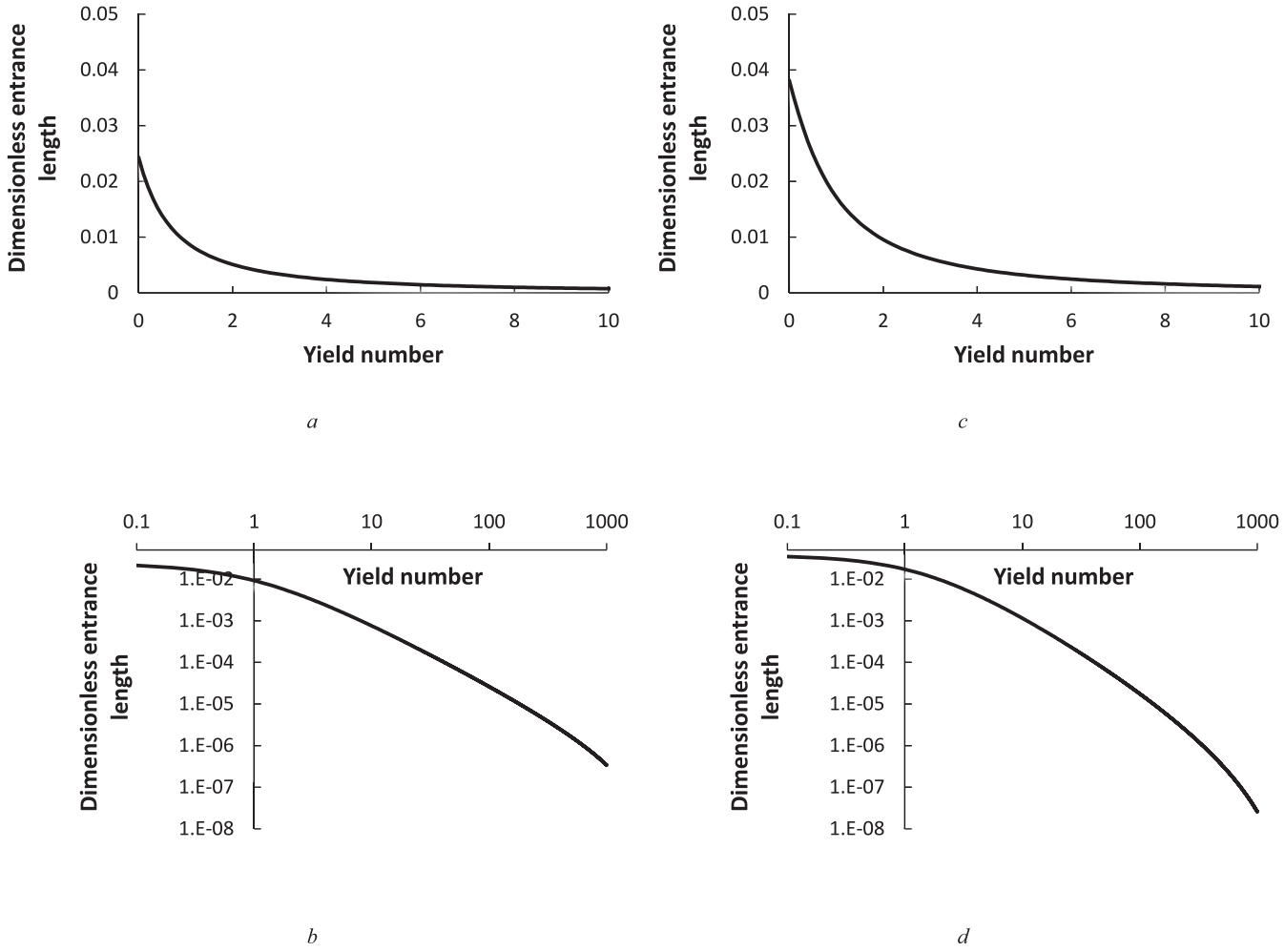

Fig. 3. Entrance length *vs.* yield number calculated using the momentum integral solution (a, b), the Batra-Kandasamy method (c, d) and the Gupta method (e, f).

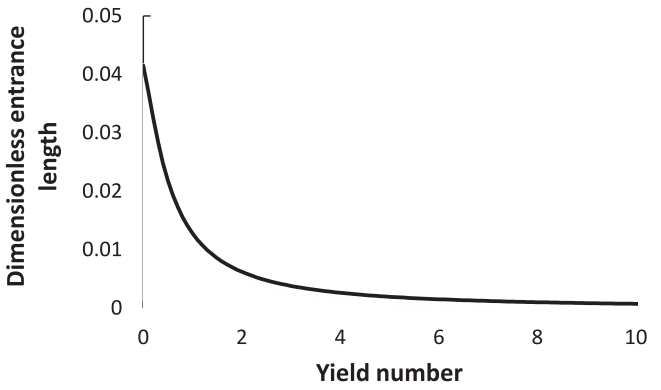

e

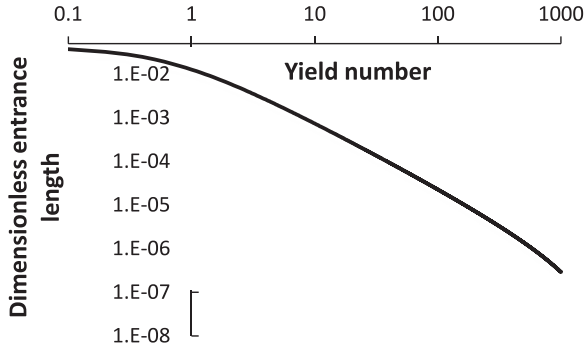

f

Fig. 3. (*continued*).

$\widehat{x}_\kappa$ *vs.* Bi, and then to use it as a diagram for a quick evaluation of $\widehat{x}_\kappa$. Constructing such plots useful for practitioners was the primary objective of this study.While working towards this objective, the ambition was to remedy a few drawbacks found in the papers from the 1990s quoted above that might adversely affect the accuracy of the calculations. In particular, the calculational recipes proposed in (Batra and Kandasamy, 1990; Gupta, 1995b) used 0.99 rather than 1 as the lower integration limit in Eq. (9). The reason for doing so was that those models were developed for a *Herschel-Bulkley* fluid, and the expressions for $\widehat{x}'(\widehat{h}_c)$ were singular at $\widehat{h}_c = 1$, resulting in an improper integral. In our study, a *Bingham* fluid is considered. In this case, it is possible to re-work expressions for $\widehat{x}'(\widehat{h}_c)$ so as to eliminate the singularity issue. It is those re-worked expressions that are represented by Eqs. (10) – (12). The re-worked expressions allow numerical integration from 1 to $\widehat{h}_{c,\kappa}$.All calculations in this study were performed using software written in C++ run on a 64-bit machine, with all variables in double precision.

3. Results

3.1. Entrance length calculated with the three methods

The results obtained with $\kappa = 0.99$, i.e. using the standard definition of the entrance length, are displayed in Fig. 3. The yield number was varied in the range from 0 to 10^3 in our calculations. Results obtained with low yield numbers (from 0 to 10) are presented in linear–linear coordinates. Results obtained with higher yield numbers are more conveniently presented in log–log coordinates. Thus, for each of the three methods described in Section 2, two plots are provided: one in linear–linear coordinates (Bi from 0 to 10) and one in log–log coordinates (Bi from 10^{-1} to 10^3). All these results are further brought together in one plot in Fig. 4. Fig. 4 suggests that the results obtained with the three methods group reasonably well in both linear–linear (Fig. 4a) and log–log (Fig. 4b) coordinates.

The ratio of the maximum and minimum entrance length predicted by the three methods was computed as a function of Bi. This ratio was found first to decrease with Bi, from 1.7 to 1.9 at around Bi = 0 to 1.1 at *Bi* = 50, then to increase from 1.1 at Bi = 50 to 13.2 at Bi = 1000. Thus, the discrepancy between the three methods becomes one order of magnitude at larger Bi. On the other hand, the entrance length might be of little practical interest at large Bi (Bi > 10) as long as the Reynolds number is sufficiently low (see also discussion in Section 5).

Another source of uncertainty in numerical prediction of entrance length is the choice of the value of κ (Section 3.2).

3.2. Entrance length: Effect of κ

In the calculations discussed in Section 3.1, the parameter κ was set equal to 0.99. As mentioned in Section 1, this value is somewhat arbitrary, setting it equal to 0.99 being common practice in this type of calculations. To examine the possible effect of this choice, two additional calculations were carried out with each of the three methods, with $\kappa = 0.98$ and $\kappa = 0.999$. The results are presented in Fig. 5. Notice the erratic behavior in the curve corresponding to $\kappa = 0.98$ as the yield

number approaches 1000. This is due to the fact that the computational accuracy deteriorates rapidly as the entrance length approaches zero. Setting κ to a smaller value means accepting a smaller value for the entrance length. A similar erratic behavior was observed also in the curve corresponding to $\kappa = 0.99$ when the calculation was extended to larger yield numbers (approaching $Bi = 10^4$, omitted in this paper).

In Fig. 5a and b the results obtained with the momentum integral solution are shown. The curves obtained with all three κ-values are close to each other (the reader is advised to discard the results obtained with $\kappa = 0.98$ at $Bi > 100$, for reasons explained above).

The largest effect of κ on the predicted entrance length is observed when the Batra-Kandasamy method is used (Fig. 5c and d). This large effect sustains at all values of the yield number.

Finally, when the Gupta method is used, the effect of κ on the predicted entrance length is noticeable (Fig. 5e and f), especially at low yield numbers ($Bi < 1$), but weaker than the one observed with the Batra-Kandasamy method.

In order to quantify the differences between the calculations with different κ-values, the ratio of the entrance lengths obtained with $\kappa = 0.999$ and $\kappa = 0.99$ was calculated for all yield number values and for each of the three entrance length evaluation methods. Let us denote this ratio λ_1 ($\lambda_1 > 1$). Moreover, the ratio of the entrance lengths obtained with $\kappa = 0.99$ and $\kappa = 0.98$ was calculated as well. Let us denote this ratio λ_2. These values are plotted *vs*. Bi in Fig. 6.

In the case of the momentum integral solution method (Fig. 6a), both ratios, λ_1 and λ_2, are relatively low and increase slightly with the yield number, i.e. the choice of κ has larger effect at larger Bi. The value of λ_1 increases from 1.06 to 1.36 as Bi increases from 0 (Newtonian limit) to 100. The value of λ_2 increases, accordingly, from 1.07 to 1.59 as *Bi* increases from 0 (Newtonian limit) to 100. Thus, increasing κ from 0.99 to 0.999 brings about only a moderate change in the calculated entrance length (36 % at $Bi = 100$, as compared to 59 % when changing κ from 0.98 to 0.99). Note that the improved accuracy of entrance length prediction achieved by increasing κ above 0.99 should be viewed in light of the discrepancies between the three methods themselves (*cf*. Fig. 4a).

When using the Batra-Kandasamy method, λ_1 varies between 1.76 and 4.77 and λ_2 varies between 1.3 and 3.67. Thus, in this case increasing κ from 0.99 to 0.999 changes the entrance length predicted at $Bi = 100$ by 377 %.

Finally, when the Gupta method is used, λ_1 and λ_2 first decrease and then increase (Fig. 6c). Their values are on the same order as those obtained with the momentum integral solution method (cf. Fig. 6a).

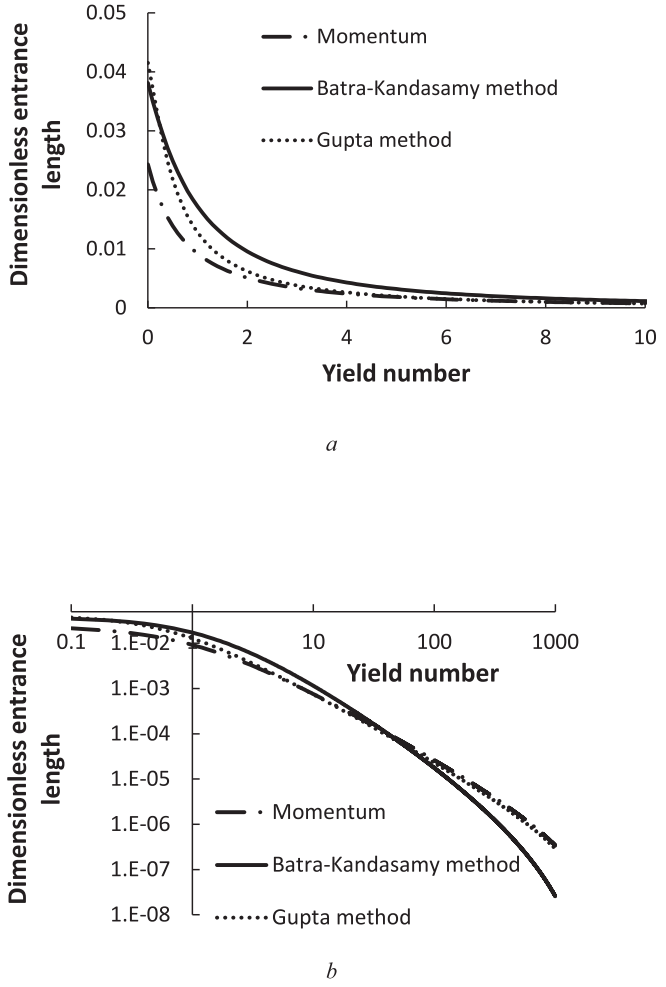

Fig. 4. Entrance length *vs*. yield number calculated using three methods plotted together: in linear–linear axes (a) and in log-linear axes (b).

4. Validity and applicability of results

The results displayed in Fig. 4 cover the range of yield number (Bingham number) from 0 to 1000. It is instructive to examine how well these results agree with the results obtained for Newtonian fluids. Several equations are available in the literature that describe the entrance length of a Newtonian fluid in a channel flow between parallel plates. We shall use two of them in this Section, *viz*. the one reported by Atkinson et al. (Atkinson et al., 1969) and the one reported by Chen (Chen, 1973). Converted to our definition of dimensionless length [Eq. (2)], Atkinson's et al. equation reads:

$$\hat{x}_{fd} = 0.088 + \frac{1.25}{\mathrm{Re}} \tag{13}$$

and Chen's equation reads:

$$\hat{x}_{fd} = 0.053 + \frac{0.79}{\mathrm{Re}(0.04\mathrm{Re} + 1)} \tag{14}$$

In Eqs. (13) and (14), Reynolds number is defined as follows: $\mathrm{Re} = 2h\rho u_0/\mu$ where ρ is the fluid density; μ is dynamic viscosity.

The momentum integral solution, the Batra-Kandasamy method and the Gupta method yield the following dimensionless entrance lengths in the Newtonian limit ($Bi = 0$): 0.0243, 0.0381 and 0.0415, respectively. Dimensionless lengths predicted by Eqs. (13), (14) and those predicted in the Newtonian limit by the three methods used in our study are plotted *vs*. Re in Fig. 7a.

Dimensionless flow distance was defined in this study through Eq. (2). This is one of the two commonly used definitions of dimensionless distance, the other being $x/2h$ or x/h which was used e.g. in (Lambride et al., 2023). The latter scalings make the dimensionless entrance length dependent on the Reynolds number. Scaling in Eq. (2) eliminates this dependency. For the sake of completeness, Fig. 7a was re-plotted in coordinates $\hat{x}_{fd}\mathrm{Re}$ *vs*. Re, i.e. effectively using the following non-dimensionalization of length: $\hat{x} = x/2h$, instead of Eq. (2). The result is displayed in Fig. 7b. In both Fig. 7a and b, the results obtained with the three methods show large deviations from both Atkinson et al. and Chen results at $\mathrm{Re} < 10$ and assume a trend similar to Atkinson et al. and Chen at $\mathrm{Re} > 30$. It can be *conjectured* that also our results obtained at $Bi \neq 0$ are only valid at Reynolds numbers above a certain threshold, and this threshold is $O(10)$. The argument above provides, of course, no *proof* of this.

The results presented in Fig. 4 are thus valid for Bi from 0 to 1000 and, likely, for Re from $n\bullet 10$ to 1000.

5. Discussion

The entrance length was defined in this study as the distance from the inlet to the location where the core velocity reaches a certain percentage of the fully developed value. This is a common ansatz used to

deal with the issue that the velocity profile only *asymptotically approaches* the fully developed profile, without ever assuming it. This ansatz is, however, not without flaws and has been debated in the literature, e.g. in (Lambride et al., 2023). This is still the area of active research in fluid mechanics, and making a contribution to this research was outside the scope of this study. The ambition here was to facilitate application of the three traditionally used methods for entrance length calculation, not to argue for or against them.

As evident in Figs. 3 to 5, the dimensionless entrance length decreases with the yield number. This is a well-known fact that can be explained as follows [cf., for instance, a similar explanation for power-law fluids provided in (Fernandes et al., 2018; Poole and Ridley, 2007)]: At higher Bi-values, the unyielded core in fully developed flow occupies a greater fraction of the of the channel's cross-section ($\widehat{h}_{c,fd}$ is larger than at lower Bi). Thus, it takes a shorter flow distance for the thickness of the unyielded core to reach $\widehat{h}_{c,fd}$ in the case when Bi is larger. (It should be remembered that the unyielded core occupies the entire cross-section at the inlet, where the velocity profile is uniform, i.e. $\widehat{h}_c$ is equal to 1 at the inlet and gradually decreases towards the fully developed value. The latter value is larger in the case of larger Bi, thus the decrease takes place over a shorter distance).

From Fig. 4b, the *dimensional* entrance length is approximately equal to the channel width when Bi = 10 and Re = 1000. Thus, in practical applications, the entrance length will be important at larger Bi-values (Bi > 10) only when Re > 1000. On the contrary, at smaller Bi-values (Bi < 10), the (dimensional) entrance length might be significant and exceed the channel width manyfold, especially if the Reynolds number is sufficiently high. When using the results obtained in this study (Fig. 4) in practice, it might therefore happen that, under the conditions of low Bi *and* high Re, the entrance length exceeds the downstream length of the channel and all flow is entry flow. (Eventually, at sufficiently high Re, transition to turbulence will begin and three methods used in this study will be invalid anyway.).

Results presented in Figs. 3, 4 call for an attempt to perform a regression. First, an exponential regression was attempted. Plotting $\log\widehat{x}_e$ *vs.* Bi showed immediately that exponential regression is not suitable in this case. Next, a two-parameter hyperbolic regression was attempted, using least squares under the constraint that the hyperbola intersect the $\widehat{x}_e$−axis at the value obtained for Newtonian fluid, i.e. with Bi = 0. These attempts failed, too. It was eventually concluded that the best way of representing the results obtained in this study is by graphs.

Sensitivity of the entrance length to the choice of κ is noticeable in all three methods. The least sensitive method in this respect is the momentum integral solution method, where increasing κ from 0.99 to 0.999 brings a change of only 6–14 % to the entrance length in the range of yield numbers from 0 to 10. The momentum integral solution method was, however, previously criticized for its low-accuracy velocity derivative evaluation (Gupta, 1995b), and the other two methods were developed in order to improve on this. These methods show, however, a higher sensitivity to the choice of κ.

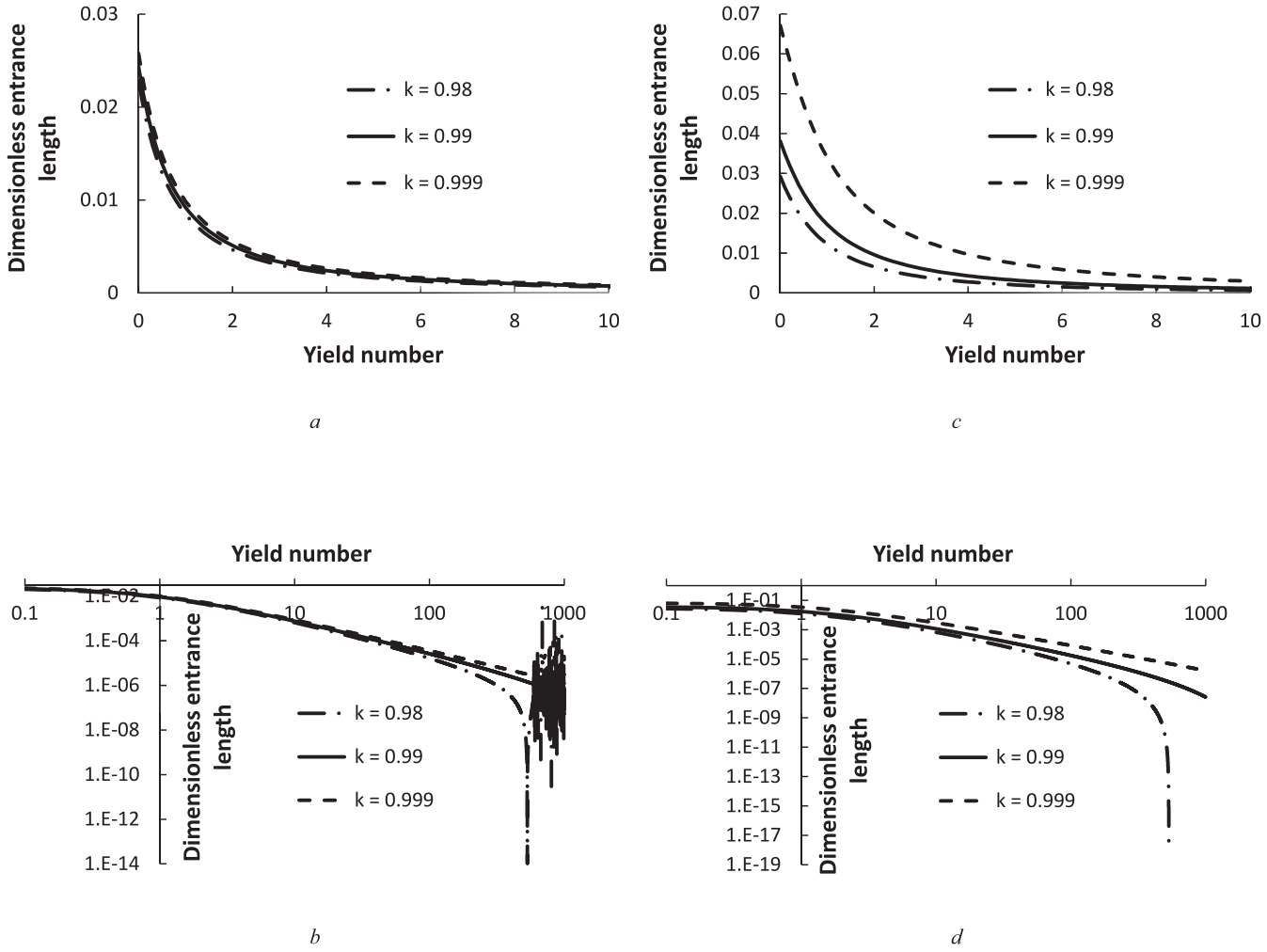

Fig. 5. Entrance length *vs.* yield number calculated with three values of κ = 0.98, 0.99 and 0.999 using the momentum integral solution (a, b), the Batra-Kandasamy method (c, d) and the Gupta method (e, f).

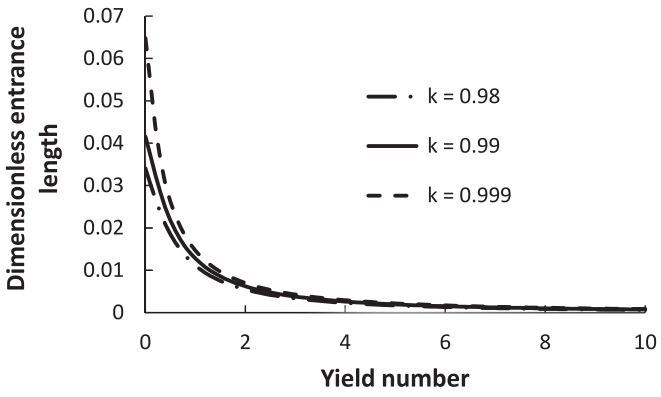

e

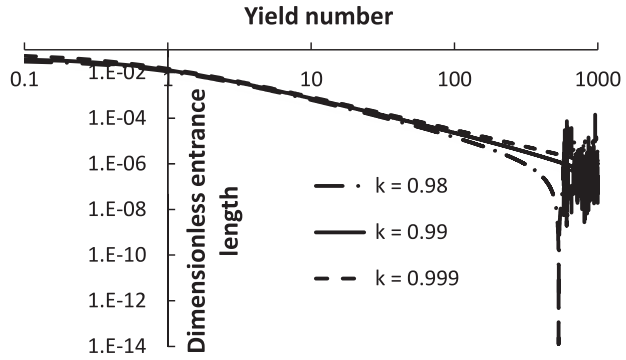

f

Fig. 5. (*continued*).

6. Conclusions

The entrance length for a Bingham fluid entering between parallel plates was calculated in this study using three well known methods. The main results, obtained with $\kappa = 0.99$ (the normal practice), are presented in Fig. 4 and are valid for yield numbers from 0 to 1000 and, most likely, for Reynolds numbers from $O(10)$ to 1000. Fig. 4 can be used for a quick estimation of the entrance length in channel flow of a Bingham fluid. The values of the entrance length calculated with the different methods group well in Fig. 4, except at relatively high yield numbers (Bi > 50) where the significance of entrance length is anyway minor (except at relatively high Re).

The calculated entrance length is quite sensitive to the choice of the parameter, κ, used in all three methods. This parameter shows what fraction of the fully developed core velocity is accepted as an approximation for the fully developed core velocity. The entrance length is thereby defined as the distance from the inlet where the core velocity reaches κ times the (theoretical) value of the core velocity in a fully developed flow. Out of the three methods, the least sensitive to κ is the momentum integral solution method: increasing κ from 0.99 (current practice) to 0.999 changes the predicted entrance length by 6 % (at Bi = 0) to 14 % (at Bi = 10). The Batra-Kandasamy method is extremely sensitive to the choice of κ, and increasing κ from 0.99 (current practice) to 0.999 would change the predicted entrance length by 76 % (at Bi = 0) to 156 % (at Bi = 10). In the Gupta method, the predicted entrance length would change by 56 % (at Bi = 0) to 14 % (at Bi = 10) if κ were increased from 0.99 (current practice) to 0.999. The findings obtained in this study suggest that the right choice of κ has a significant impact that cannot be neglected in some applications (while it can be in others where only a crude estimate of the entrance length is required). Methods and criteria for entrance length calculation need further research in order to reduce the errors, discrepancies between calculation methods, and the degree of arbitrariness (i.e. the sensitivity to the chosen value of κ).

CRediT authorship contribution statement

Alexandre Lavrov: Writing – original draft, Visualization, Software, Methodology, Investigation, Formal analysis, Data curation, Conceptualization.

Declaration of competing interest

The authors declare that they have no known competing financial interests or personal relationships that could have appeared to influence the work reported in this paper.

Data availability

No data was used for the research described in the article.

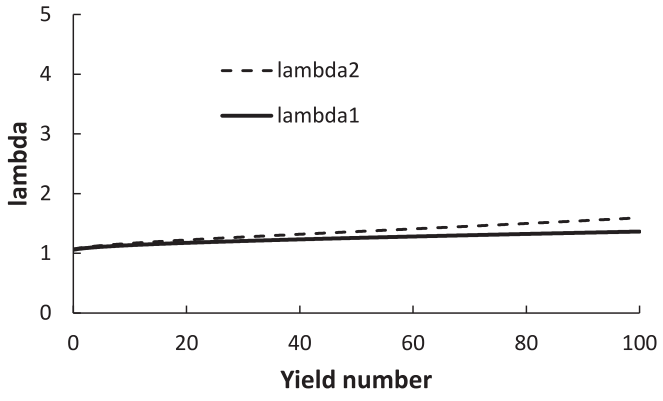

a

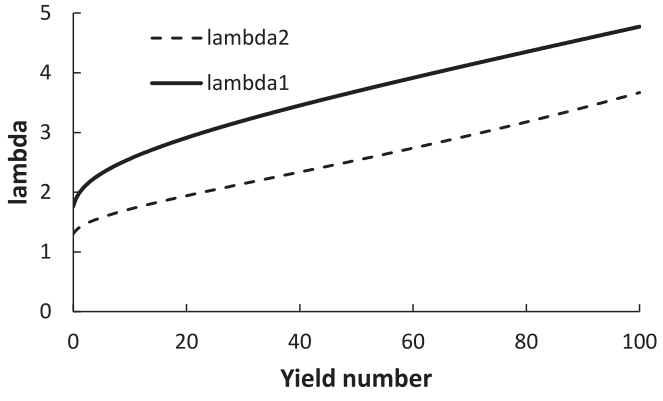

b

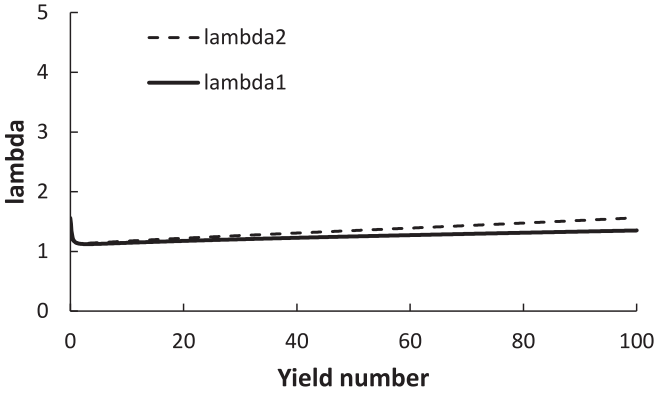

c

Fig. 6. $\lambda_{1,2}$ *vs.* yield number calculated using the momentum integral solution (a), the Batra-Kandasamy method (b) and the Gupta method (c).

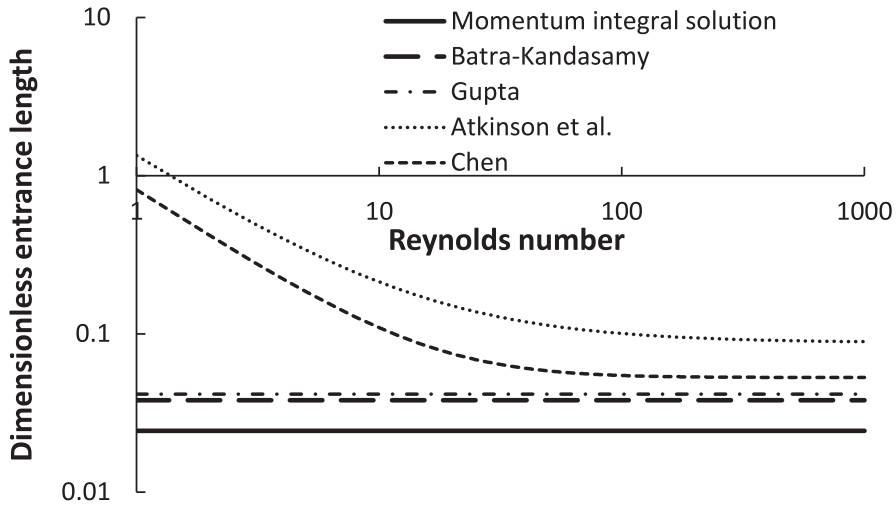

a

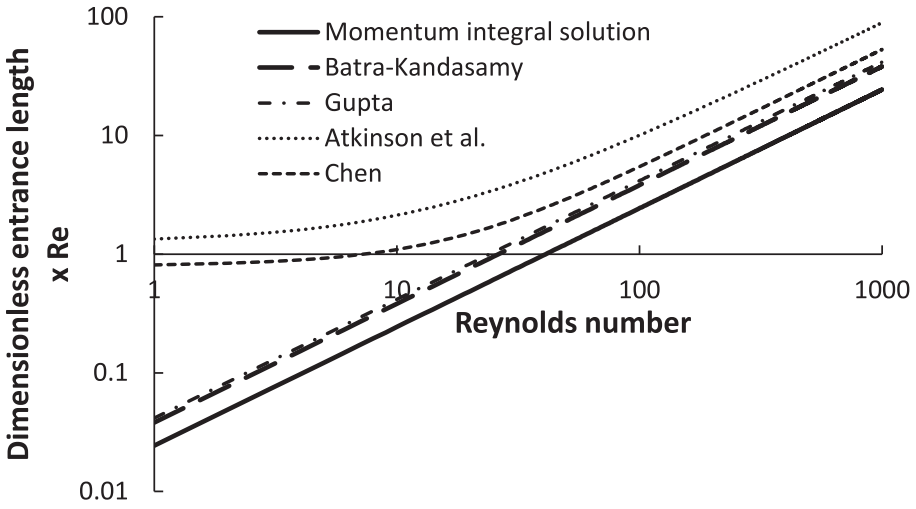

b

Fig. 7. Dimensionless entrance length (a) and dimensionless entrance length times Reynolds number (b) *vs*. Re obtained in the Newtonian limit (Bi = 0).

Acknowledgement

The author is grateful to the anonymous reviewers for valuable comments and suggestions that helped to improve the manuscript during the revision.

References

Atkinson, B., Brocklebank, M.P., Card, C.C.H., Smith, J.M., 1969. Low Reynolds number developing flows. AIChE J 15, 548–553.
Batra, R.L., Kandasamy, A., 1990. Entrance flow of Herschel-Bulkley fluids in a duct. Fluid Dyn. Res. 6, 43–50.
Chen, R.-Y., 1973. Flow in the entrance region at low Reynolds numbers. J. Fluids Eng. 95, 153–158.
Das, B., 1992. Entrance region flow of the Hershel-Bulkley fluid in a circular tube. Fluid Dyn. Res. 10, 39.
Fernandes, C., Ferrás, L.L., Araujo, M.S., Nóbrega, J.M., 2018. Development length in planar channel flows of inelastic non-Newtonian fluids. J. Nonnewton. Fluid Mech. 255, 13–18.
Gupta, R.C., 1987. Laminar two-dimensional entrance region flow of power-law fluids. Acta Mech. 67, 129–137.
Gupta, R.C., 1995a. Developing Bingham fluid flow in a channel. Math. Comput. Model. 21, 21–28.
Gupta, R.C., 1995b. Herschel-Bulkley fluid flow development in a channel. Polym.-Plast. Technol. Eng. 34, 475–492.
Hanks, R.W., 1963. The laminar-turbulent transition for fluids with a yield stress. AIChE J 9, 306–309.
Lambride, C., Syrakos, A., Georgiou, G.C., 2023. Entrance length estimates for flows of power-law fluids in pipes and channels. J. Nonnewton. Fluid Mech. 317, 105056.
Lipscomb, G.G., Denn, M.M., 1984. Flow of bingham fluids in complex geometries. J. Nonnewton. Fluid Mech. 14, 337–346.
Mitsoulis, E., Huilgol, R.R., 2004. Entry flows of Bingham plastics in expansions. J. Nonnewton. Fluid Mech. 122, 45–54.
Nowak, Z., Gajdeczko, B., 1983. Laminar entrace region flow of the Bingham fluid. Acta Mech. 49, 191–200.
Poole, R.J., Ridley, B.S., 2007. Development-length requirements for fully developed laminar pipe flow of inelastic non-Newtonian liquids. J. Fluids Eng. 129, 1281–1287.
Rodríguez de Castro, A., Ahmadi-Sénichault, A., Omari, A., 2020. Determination of the aperture distribution of rough-walled rock fractures with the non-toxic Yield Stress fluids porosimetry method. Adv. Water Resour. 146, 103794.
Soto, R.J., Shah, V.L., 1976. Entrance flow of a yield-power law fluid. Appl. Sci. Res. 32, 73–85.
Wilson, S.D.R., Taylor, A.J., 1996. The channel entry problem for a yield stress fluid. J. Nonnewton. Fluid Mech. 65, 165–176.